Electronic Supplementary Material (ESI) for Journal of Materials Chemistry C.
This journal is © The Royal Society of Chemistry 2022

A {Zn_4} cluster as a bi-functional luminescence sensor for highly sensitive detection of chloride ion and histidine in aqueous media

Jing Li, Ke-Xin Ma, Yan Yang, Hua Yang, Jing Lu, Da-Cheng Li, Jian-Min Dou, Hui-Yan Ma,* Su-Na Wang* and Yun-Wu Li*

Shandong Provincial Key Laboratory of Chemical Energy Storage and Novel Cell Technology, and School of Chemistry and Chemical Engineering, Liaocheng University, Liaocheng 252000, P. R. China.

E-mails: mahuiyanyan@163.com; wangsuna@lcu.edu.cn; liyunwu@lcu.edu.cn.

Table S1 Crystal data and structure refinement parameters for the **{Zn_4}** cluster.

Complex		**{Zn_4}**	
Formula	$C_{48}H_{46}Cl_2N_{20}O_{12}Zn_4$	γ [°]	90.00
F_w	1427.43	V (Å3)	2931.0(2)
λ/Å	1.54178	Z	2
T/K	298.15	Dc/Mg/m^3	1.617
Crystal system	Monoclinic	F(000)	1448.0
Space group	P12$_1$/c1	Reflections collected/unique	10918/5112
a [Å]	10.1349(5)	Rint	0.0560
b [Å]	19.5541(8)	Data/Restraints/Parameters	5112/1118/388
c [Å]	15.0215(7)	$R1$/wR_2 [$I>2\sigma(I)$][a]	0.0693/0.1957
α[°]	90.00	$R1$/wR_2 [(all data)][b]	0.1140/0.2270
β[°]	100.074(5)	GOF on F^2	1.030

[a] $R_1 = \Sigma(||F_0| - |F_C||)/\Sigma|F_0|$; [b] $wR_2 = [\Sigma w(|F_0|^2 - |F_C|^2)^2/(\Sigma w|F_0|^2)^2]^{1/2}$.

Table S2 The selected bond lengths [Å] and angles [°] of the **{Zn_4}** cluster.

N(9)-Zn(1)#1	2.286(6)	Zn(1)-N(1)	2.001(6)
N(7)-Zn(1)#1	2.015(6)	Zn(2)-Cl(1)	2.187(2)
Zn(1)-Zn(1)#1	3.160(2)	Zn(2)-O(3)	2.015(4)
Zn(1)-O(3)	2.051(5)	Zn(2)-N(6)	2.023(6)
Zn(1)-O(3)#1	2.160(5)	Zn(2)-N(2)	1.993(6)
C(15)-N(9)-Zn(1)#1	129.4(5)	C(14)-N(9)-Zn(1)#1	113.3(5)
C(13)-N(7)-Zn(1)#1	121.3(5)	N(6)-N(7)-Zn(1)#1	131.4(4)
N(9)#1-Zn(1)-Zn(1)#1	136.96(18)	N(7)#1-Zn(1)-N(9)#1	73.7(2)
N(7)#1-Zn(1)-Zn(1)#1	107.00(17)	N(7)#1-Zn(1)-O(3)#1	87.4(2)
N(7)#1-Zn(1)-O(3)	119.8(2)	O(3)#1-Zn(1)-N(9)#1	158.9(2)
O(3)-Zn(1)-N(9)#1	98.2(2)	O(3)#1-Zn(1)-Zn(1)#1	40.08(13)
O(3)-Zn(1)-Zn(1)#1	42.70(13)	O(3)-Zn(1)-O(3)#1	82.79(19)
N(1)-Zn(1)-N(9)#1	99.4(2)	N(1)-Zn(1)-N(7)#1	149.4(3)
N(1)-Zn(1)-Zn(1)#1	98.26(18)	N(1)-Zn(1)-O(3)#1	101.7(2)
N(1)-Zn(1)-O(3)	90.4(2)	O(3)-Zn(2)-Cl(1)	112.74(15)
O(3)-Zn(2)-N(6)	98.9(2)	N(6)-Zn(2)-Cl(1)	123.62(18)
N(2)-Zn(2)-Cl(1)	117.17(19)	N(2)-Zn(2)-O(3)	95.7(2)
N(2)-Zn(2)-N(6)	103.9(2)	Zn(1)-O(3)-Zn(1)#1	97.21(19)
Zn(2)-O(3)-Zn(1)	111.9(2)	Zn(2)-O(3)-Zn(1)#1	110.3(2)
N(7)-N(6)-Zn(2)	107.6(4)	C(18)-N(6)-Zn(2)	144.9(5)
C(6)-N(2)-Zn(2)	139.5(5)	N(1)-N(2)-Zn(2)	114.3(4)
N(2)-N(1)-Zn(1)	125.3(5)	C(1)-N(1)-Zn(1)	127.5(5)

Symmetry transformations used to generate equivalent atoms: #1: -x+1, -y+1, -z+1.

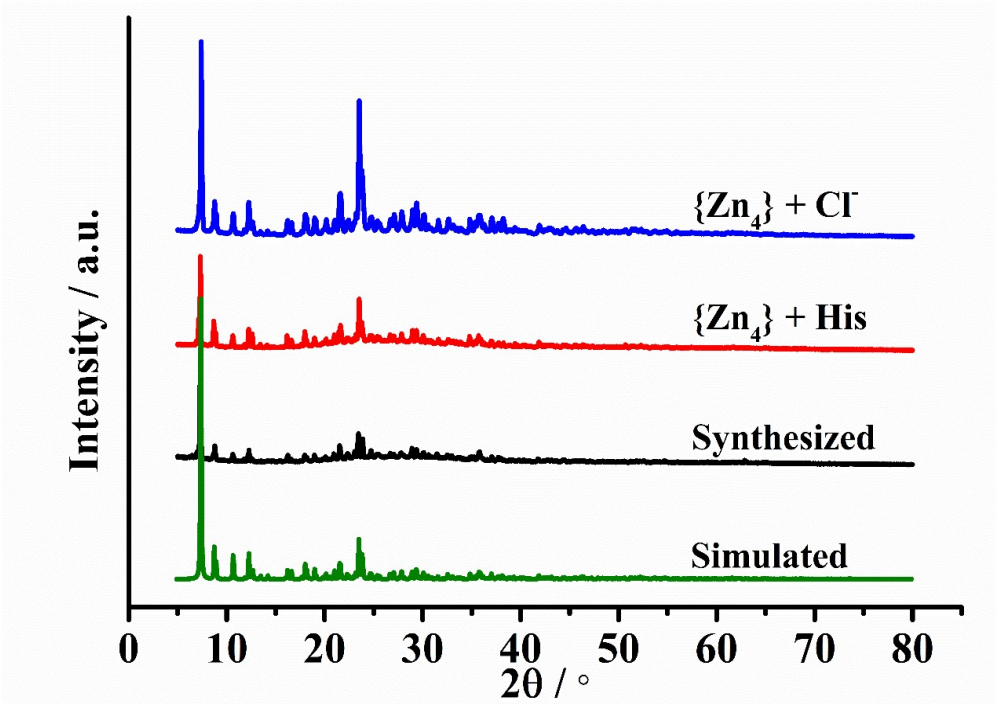

Fig. S1 PXRD of the **{Zn$_4$}** cluster after being immersed in aqueous solutions of Cl$^-$ and His for 3 days.

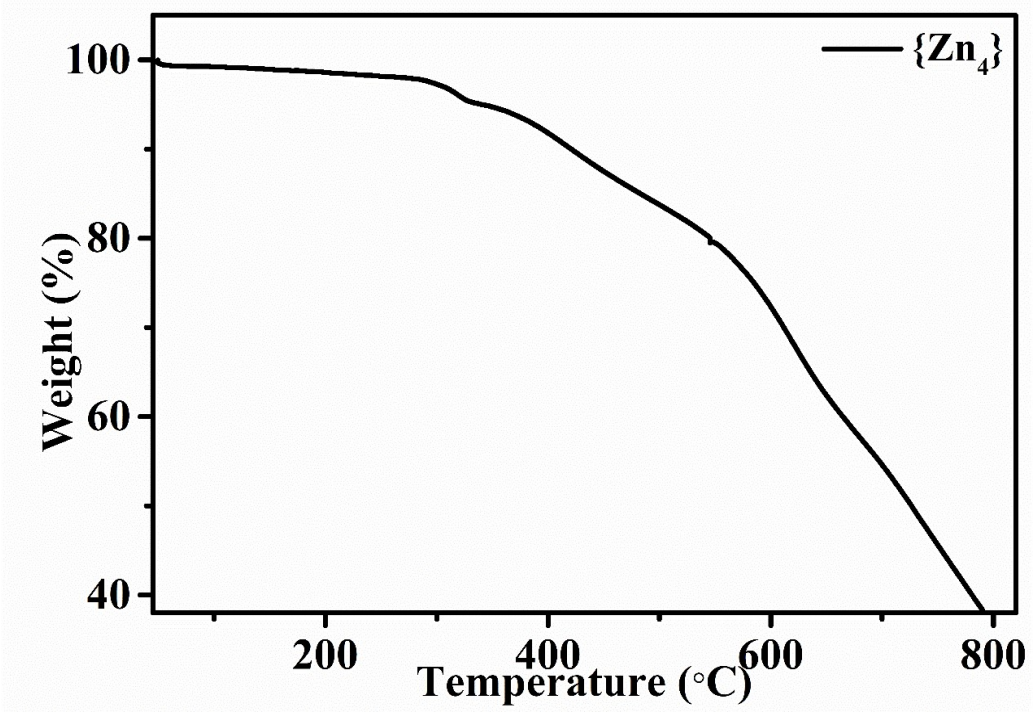

Fig. S2 The TGA curve of the **{Zn$_4$}** cluster.

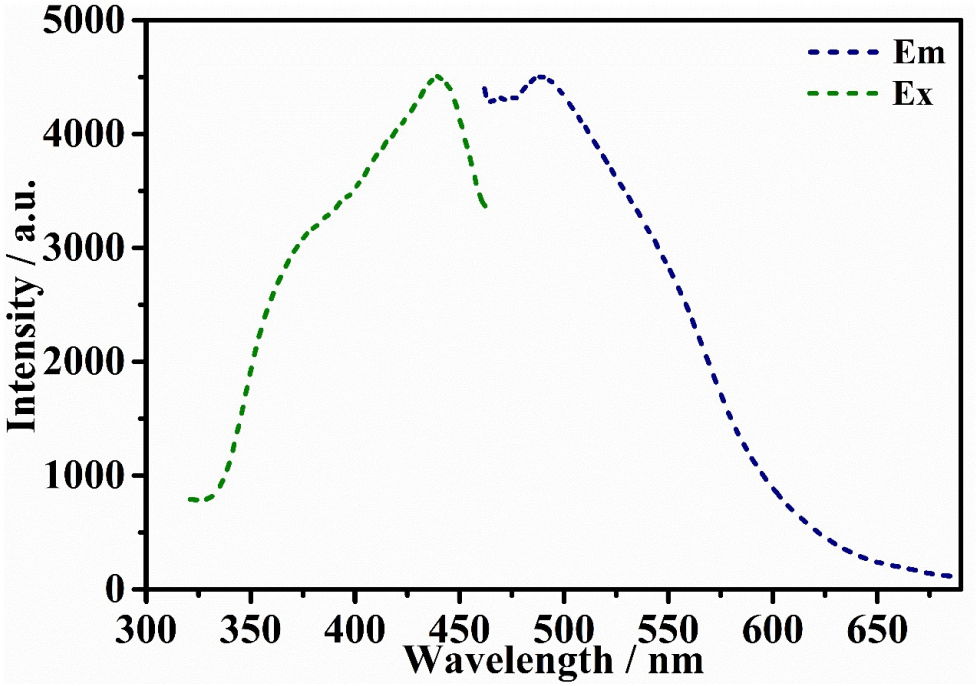

Fig. S3 Excitation and emission spectra of free Opt ligand.

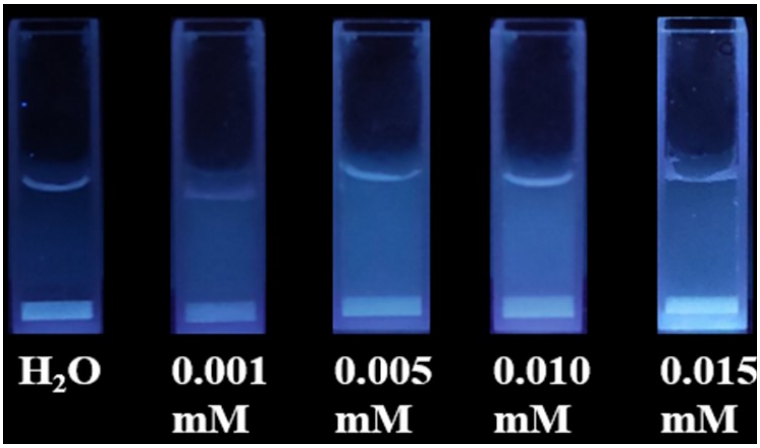

Fig. S4 Luminescence pictures of the **{Zn_4}** cluster in the presence of different concentrations of Cl^- under 365 nm UV lamp.

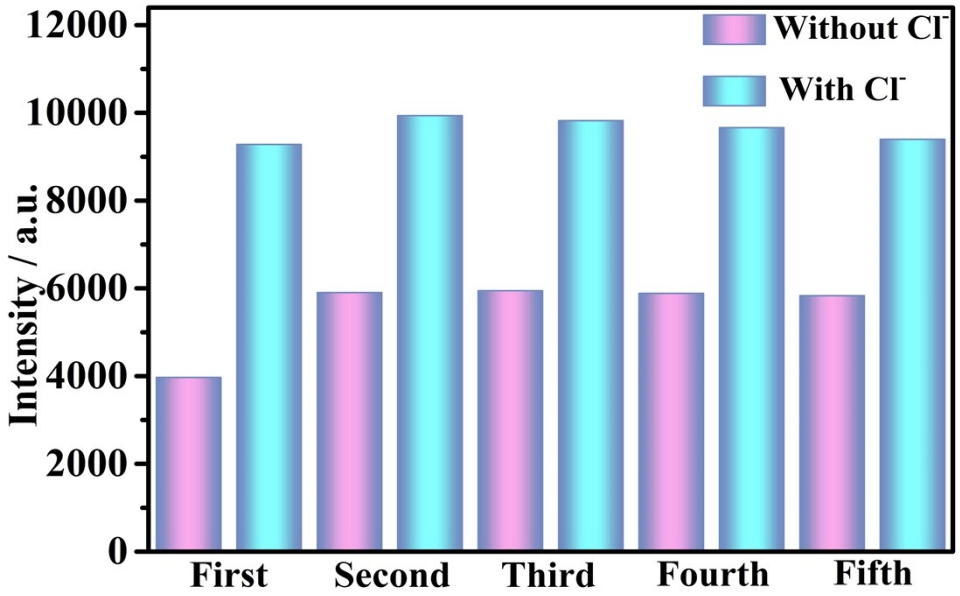

Fig. S5. The luminescence intensity of the **{Zn_4}** cluster after five sensing cycles for Cl^-.

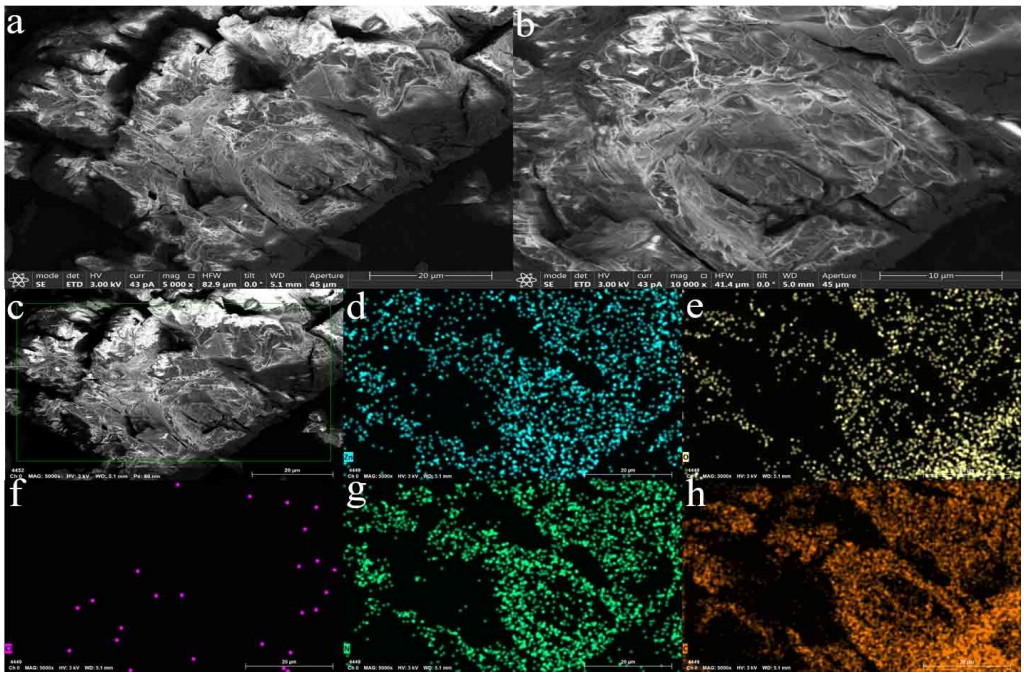

Fig. S6 (a)-(c) SEM images of the **{Zn_4}** cluster. (d)-(h) EDS mapping images of selected regions: Zn, O, Cl, N and C.

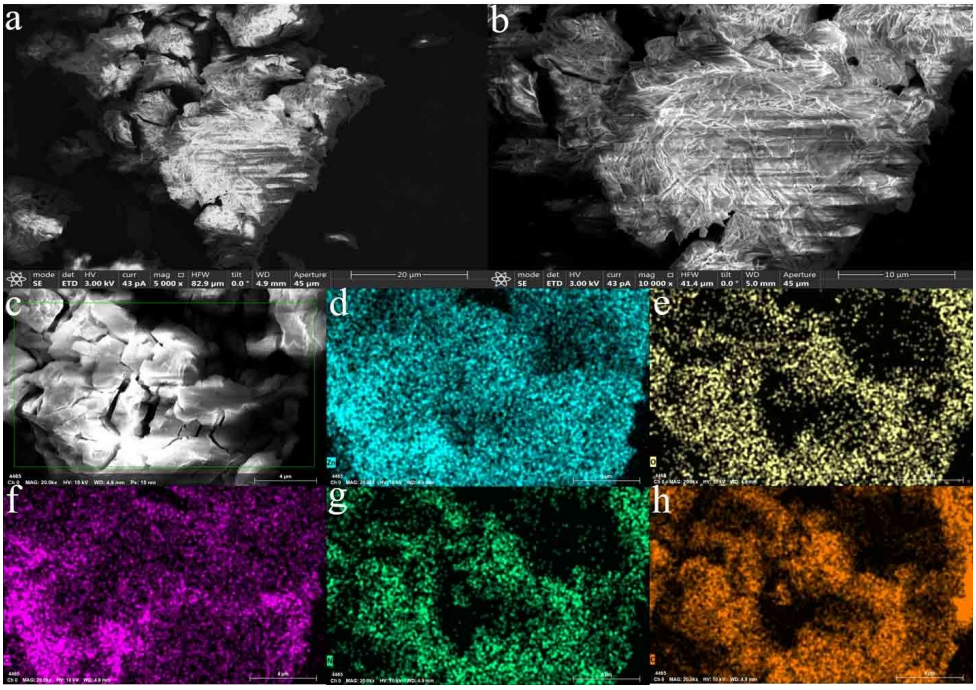

Fig. S7 (a)-(c) SEM images of the **{Zn_4}** cluster treated with 1 mM aqueous solution of Cl^-. (d)-(h) EDS mapping images of selected regions: Zn, O, Cl, N and C.

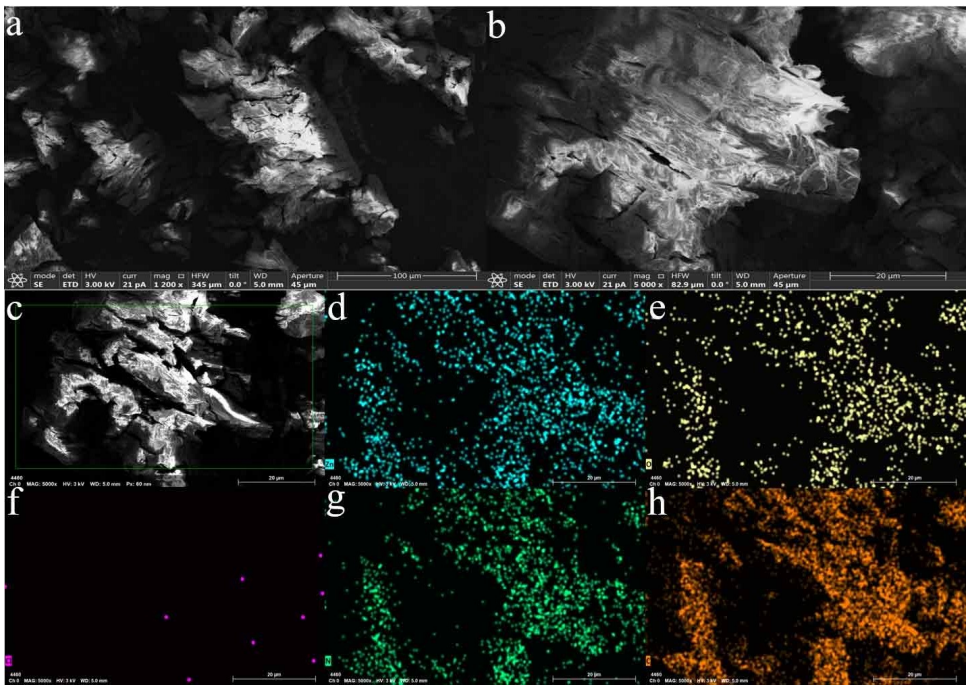

Fig. S8 (a)-(c) SEM images of the **{Zn_4}** cluster treated with 1 mM aqueous solution of His. (d)-(h) EDS mapping images of selected regions: Zn, O, Cl, N and C.

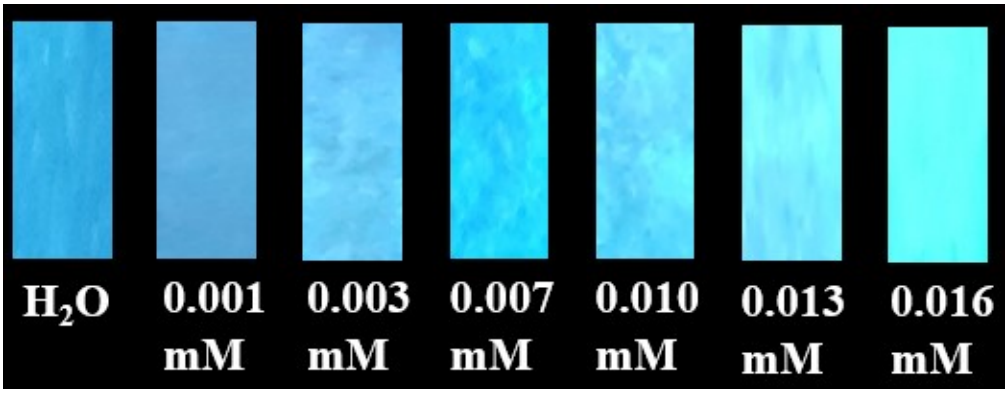

Fig. S9 Luminescent test paper pictures of the **{Zn$_4$}** cluster in the presence of different concentrations of Cl^- under 365 nm UV lamp.

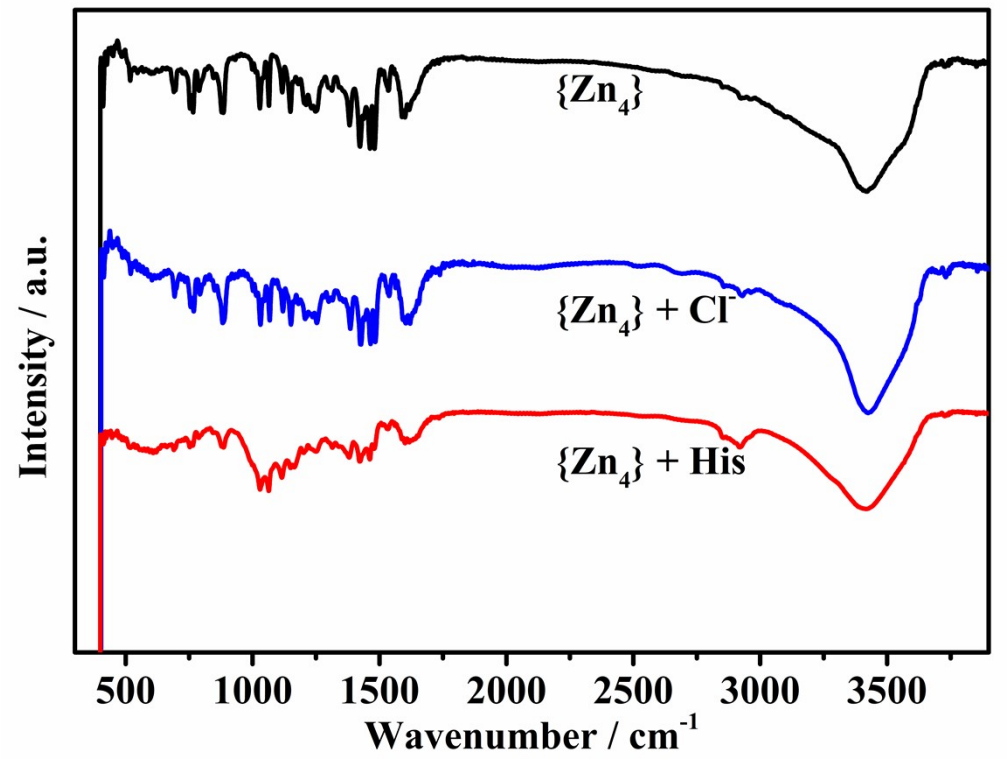

Fig. S10 IR spectra of the **{Zn$_4$}** cluster after being immersed in aqueous solutions of Cl^- and His for 3 days.

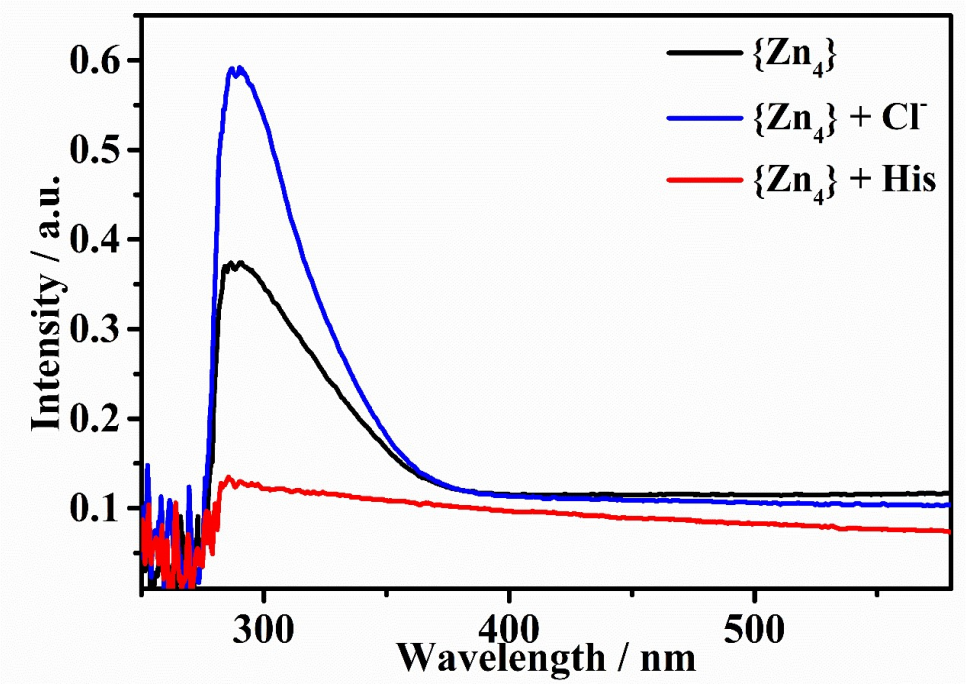

Fig. S11 UV-vis spectra of the **{Zn_4}** cluster after being immersed in aqueous solutions of Cl^- and His for 3 days.

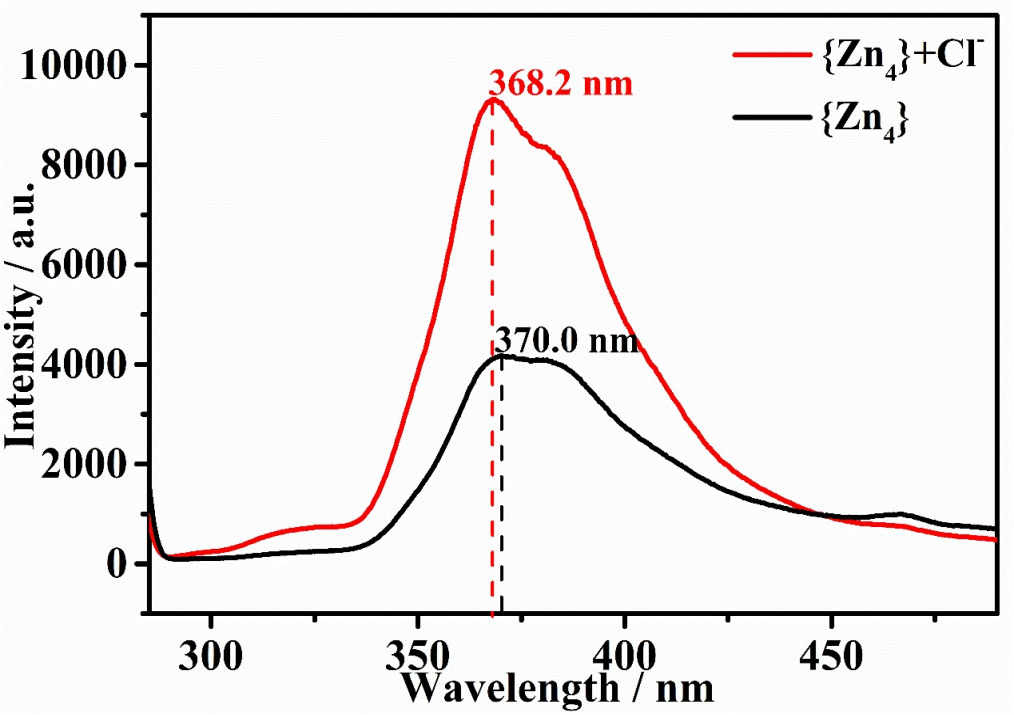

Fig. S12 Luminescence emission spectra of the **{Zn_4}** cluster before and after sensing.

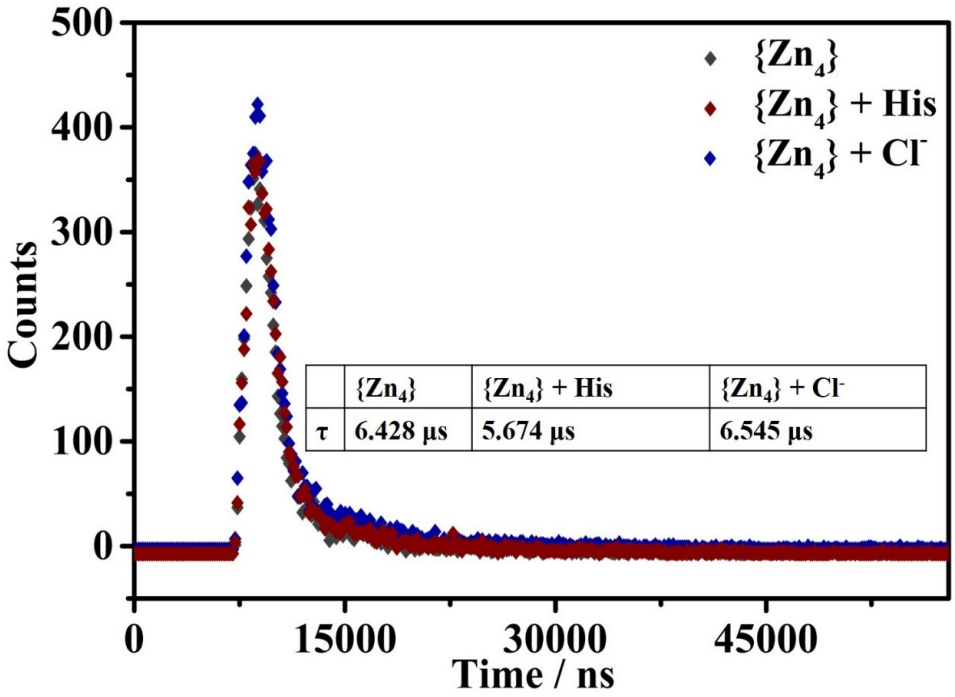

Fig. S13 The luminescence decay lifetimes of the **{Zn$_4$}** cluster after being immersed in aqueous solutions of Cl^- and His for 3 days.

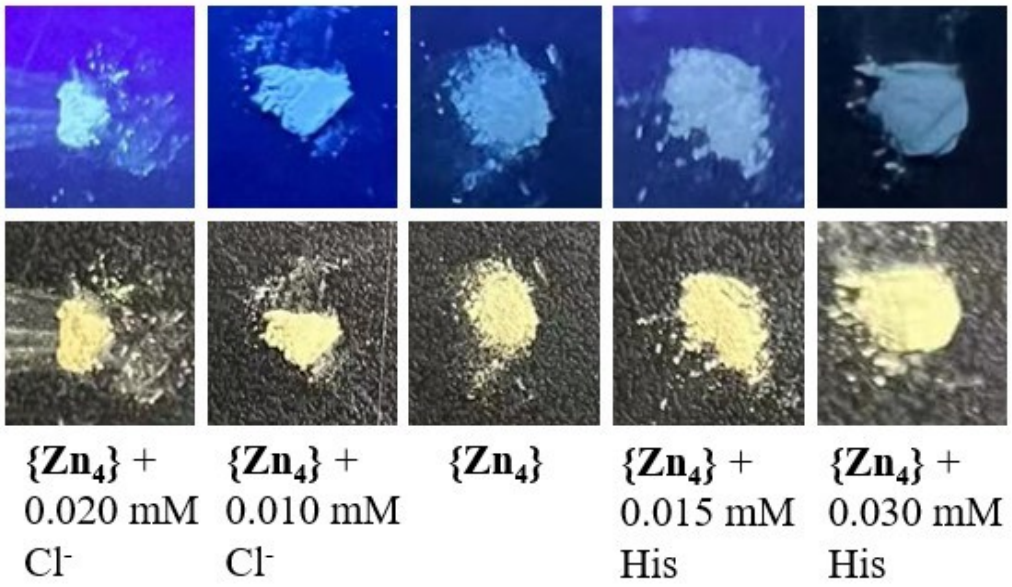

Fig. S14 Photos of the **{Zn$_4$}** cluster soaked in different concentrations of Cl^-/His aqueous solutions under 365 nm UV lamp.

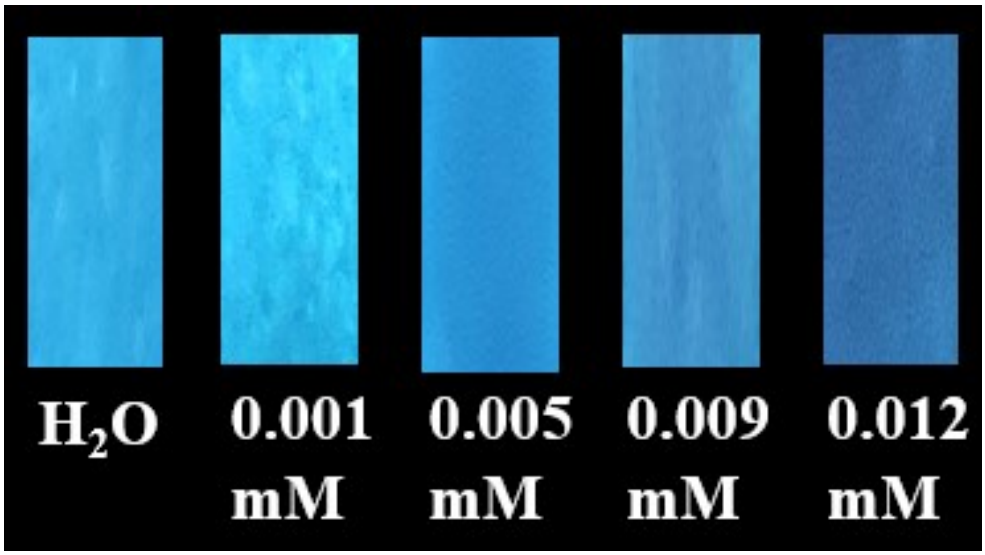

Fig. S15 Luminescent test paper pictures in the presence of different concentrations of His under 365 nm UV lamp.

Table S3. Performance comparison among different analysis methods for probing Cl^-.

Cl^-				
Sensor	LODs/μM	Medium	Method	Refs.
The {**Zn_4**} cluster	0.94	H_2O	Fluorescent	This work
Ag NWs/Pt/GCE	20	-	Electroanalytical	S1
3D-GN/CPE	200	-	Electroanalytical	S2
QG@MA-Ag/GCE	0.16	-	Electroanalytical	S3
M2	19	H_2O	Fluorescent	S4
BeQ_2	66	NaCl	Fluorescent	S5
Ag-PCN	60	H_2O	Fluorescent	S6
THPP	7.5	HEPES	Fluorescent	S7
MQ-DS	180	phosphate-citric acid buffer	Fluorescent	S8
$CsPbBr_3$ PQDs/cellulose	4110	H_2O	Colorimetric	S9
Ag^+-FBI	19	HEPES buffer solution containing 10% DMSO	Fluorescent	S10
MQAF	16700	HEPES buffer solution	Fluorescent	S11

Table S4. The element ratio of the **{Zn_4}** cluster untreated and treated with Cl^- or His aqueous solution.

System	Zn/%	Cl/%	O/%	N/%	C/%
{Zn_4} cluster	19.67	3.93	9.2	22.7	44.5
{Zn_4} cluster + Cl^-	20.99	7.67	7.99	20.93	42.42
{Zn_4} cluster + His	18.36	3.66	9.33	23.84	44.81

Table S5. The E_{HOMO}, E_{LUMO} and ΔE of various ion systems.

System	Zn1-Opt	Zn1-Opt +Cl^-	Zn1-Opt +F^-	Zn1-Opt +Br^-	Zn1-Opt +I^-	Zn1-Opt +OH^-	Zn1-Opt +SCN^-
E_{HOMO} (a.u.)	-3.77787	-0.22974	-0.54086	-0.22488	0.02255	-0.39566	-0.23466
ΔE (a.u.)	0.02662	0.01400	0.01718	0.01511	0.02255	0.03726	0.0143
E_{LUMO} (a.u.)	-0.35125	-0.21574	-0.52368	-0.20977	1.00400	-0.35840	-0.22036

Table S6. Performance comparison among different analysis methods for probing His.

Histidine				
Sensor	LODs/μM	Medium	Method	Refs.
{Zn_4} cluster	0.83	H_2O	Fluorescent	This work
$HPOx_2$	10	H_2O	Chiroptical	S12
complex LAl^{3+}	0.6	HEPES buffer	Fluorescent	S13
Eu-MOF	100	H_2O	Fluorescent	S14
BINOL-Zn	0.35	DMF/1%, phosphate buffer	Fluorescent	S15
CCS	7.64	high water-content solution	Fluorescent	S16
Co-ETTB	11	50% THF aqueous solution	Fluorescent	S17
CAQA	26	aqueous ACN-HEPES buffer solution	Fluorescent	S18
CuL^1	10	DMSO/H_2O (1:9, v/v)	Fluorescent	S19
Cu(pydxsemicarbazide)Cl_2	1.9	aqueous HEPES buffer	Fluorescent	S20

References

(S1) X. Qin, H. Wang, Z. Miao, X. Wang, Y. Fang, Q. Chen and X. Shao, Synthesis of Silver Nanowires and Their Applications in the Electrochemical Detection of Halide. *Talanta*, 2011, **84**, 673–678.

(S2) M. Zhang, C. Wang, Z. Zhang, J. Ye and P. Fang, A Novel Carbon Paste Electrode for Sensitive, Selective and Rapid Electrochemical Determination of Chloride Ion Based on Three-Dimensional Graphene. *Sensor. Actuat. B-Chem.*, 2019, **299**, 126951.

(S3) Y. Wan, Y. Hua, M. Liu, S. Li, M. Yin, X. Lv and H. Wang, Highly Selective Electroanalysis for Chloride Ions by Conductance Signal Outputs of Solid-State AgCl Electrochemistry Using Silver-Melamine Nanowires. *Sensor. Actuat. B-Chem.*, 2019, **300**, 127058.

(S4) C. Ma, F. Y. Zhang, Y. Y. Wang, X. Y. Zhu, X. Y. Liu, C. Y. Zhao and H. X. Zhang, Synthesis and Application of Ratio Fluorescence Probe for Chloride. *Anal. Bioanal. Chem.*, 2018, **410**, 6507–6516.

(S5) F. Y. Zhang, C. Ma, Y. Y. Wang, W. Liu, X. Y. Liu and H. X. Zhang, Fluorescent Probes for Chloride Ions in Biological Samples. *Spectrochim. Acta A.*, 2018, **205**, 428–434.

(S6) Z. S. Zhang, Y. Gao, P. Li, B. H. Qu, Z. Y. Mu, Y. Liu, Y. Qu, D. G. Kong, Q. Chang and L. Q. Jing, Highly Sensitive Fluorescence Detection of Chloride Ion in Aqueous Solution with Ag-Modified Porous g-C_3N_4 Nanosheets. *Chin. Chem. Lett.*, 2020, **31**, 2725–2729.

(S7) F. Y. Zhang, C. Ma, Z. J. Jiao, S. Mu, Y. D. Zhang, X. Y. Liu and H. X. Zhang, A NIR Turn-on Fluorescent Sensor for Detection of Chloride Ions in Vitro and in Vivo. *Spectrochim. Acta A.*, 2020, **228**, 117729.

(S8) P. Li, S. Zhang, N. Fan, H. Xiao, W. Zhang, W. Zhang, H. Wang and B. Tang, Quantitative Fluorescence Ratio Imaging of Intralysosomal Chloride Ions with Single Excitation/Dual Maximum Emission. *Chem. Eur. J.*, 2014, **20**, 11760–11767.

(S9) B. Park, S. M. Kang, G. W. Lee, C. H. Kwak, M. Rethinasabapathy and Y. S.

Huh, Fabrication of $CsPbBr_3$ Perovskite Quantum Dots/Cellulose-Based Colorimetric Sensor: Dual-Responsive On-Site Detection of Chloride and Iodide Ions. *Ind. Eng. Chem. Res.*, 2020, **59**, 793−801.

(S10) J. Kim, S. J. Lee, S. Kim, M. Jung, H. Lee and M. S. Han, Development of A Fluorescent Chemosensor for Chloride Ion Detection in Sweat Using Ag^+-Benzimidazole Complexes. *Dyes Pigm.*, 2020, **177**, 108291.

(S11) P. Li, T. Xie, N. N. Fan, K. X. Li and B. Tang, Ratiometric Fluorescence Imaging for Distinguishing Chloride Concentration Between Normal and Ischemic Ventricular Myocytes. *Chem. Commun.*, 2012, **48**, 2077–2079.

(S12) K. Liu, G. Du, L. Ye and L. Jiang, A Chiroptical Nanoprobe for Highly Selective Recognition of Histidine Enantiomers in Aqueous Media. *Sensor. Actuat. B-Chem.*, 2019, **284**, 55–62.

(S13) E. Oliveira, C. Santos, P. Poeta, J. L. Capelo and C. Lodeiro, Turn-on Selective Vitamin B6 Derivative Fluorescent Probe for Histidine Detection in Biological Samples. *Analyst*, 2013, **138**, 3642–3645.

(S14) A. F. Yang, S. L. Hou, Y. Shi, G. L. Yang, D. B. Qin and B. Zhao, Stable Lanthanide-Organic Framework As A Luminescent Probe to Detect Both Histidine and Aspartic Acid in Water. *Inorg. Chem.*, 2019, **58**, 6356–6362.

(S15) Y. Mao, M. A. Abed, N. B. Lee, X. Wu, G. Du and L. Pu, Determining the Concentration and Enantiomeric Composition of Histidine Using One Fluorescent Probe. *Chem. Commun.*, 2021, **57**, 587–590.

(S16) A. Pundi, C. J. Chang, J. Chen, S. R. Hsieh and M. C. Lee, A Chiral Carbazole Based Sensor for Sequential "On-Off-On" Fluorescence Detection of Fe^{3+} and Tryptophan/histidine. *Sensor. Actuat. B-Chem.*, 2021, **328**, 129084.

(S17) X. L. Guo, N. S. Zhu, S. P. Wang, G. H. Li, F. Q. Bai, Y. Li, Y. H. Han, B. Zou, X. B. Chen, Z. Shi and S. H. Feng, Stimuli-Responsive Luminescent Properties of Tetraphenylethene-Based Strontium and Cobalt Metal–Organic Frameworks. *Angew. Chem. Int. Ed.*, 2020, **59**, 19716–19721.

(S18) Q. H. You, A. W. M. Lee, W. H. Chan, X. M. Zhu and K. C. F. Leung, A Coumarin-Based Fluorescent Probe for Recognition of Cu^{2+} and Fast Detection of

Histidine in Hard-To-Transfect Cells by a Sensing Ensemble Approach. *Chem. Commun.*, 2014, **50**, 6207–6210.

(S19) D. Wang, J. Q. Zheng, X. J. Zheng, D. C. Fang, D. Q. Yuan and L. P. Jin, A Fluorescent Chemosensor for the Sequential Detection of Copper (II) and Histidine and Its Biological Applications. *Sensor. Actuat. B-Chem.*, 2016, **228**, 387–394.

(S20) C. Das, B. Pakhira, A. L. Rheingold and S. K. Chattopadhyay, Turn on ESIPT Based Chemosensor for Histidine: Application in Urine Analysis and Live Cell Imaging. *Inorg. Chim. Acta*, 2018, **482**, 292–298.